Nuclear Instruments and Methods in Physics Research A 610 (2009) 253–257

Contents lists available at ScienceDirect

Nuclear Instruments and Methods in Physics Research A

journal homepage: www.elsevier.com/locate/nima

# Investigation of the secondary emission characteristics of CVD diamond films for electron amplification

J.S. Lapington [a,*], D.P. Thompson [a], P.W. May [b], N.A. Fox [b], J. Howorth [c], J. Milnes [c], V. Taillandier [d]

[a] Space Research Centre, Univeristy of Leicester, Leicester LE1 7RH, UK
[b] Department of Chemistry, Univeristy of Bristol, Bristol BS8 1TS, UK
[c] Photek Ltd., St. Leonards on Sea, East Sussex TN38 9NS, UK
[d] Commissariat a l'Energie Atomique, SPN Bruyeres-le-Chatel, 91297 Arpajon Cedex, France

ARTICLE INFO

Available online 12 June 2009

*Keywords:*
CVD diamond
Dynode
Secondary electron emission
Photomultiplier
Detector

ABSTRACT

Chemical vapour deposition (CVD) diamond offers great potential as a low-cost, high-yield, easily manufactured secondary electron emitter for electron multiplication in devices such as photomultiplier tubes. Its potential for high secondary electron yield offers several significant benefits for these devices including higher time resolution, faster signal rise time, reduced pulse height distribution, low noise, and chemical stability.

We describe an experiment to characterize the secondary emission yield of CVD diamond manufactured using different processes and process parameters and discuss the degradation of secondary electron yield and experimental difficulties encountered due to unwanted electron beam-induced contamination. We describe techniques utilized to overcome these difficulties, and present measurements of secondary yield from CVD diamond dynodes in reflection mode.

We discuss the application of CVD diamond dynode technology, both in reflection and transmission mode, to advanced high-speed imaging and photon-counting detectors and describe future plans in this area.



## 1. Introduction

Despite the widespread success of solid-state imaging devices such as the ubiquitous CCD, there are many fields where the sensitivity to detect single-quanta accurately in time and space is required, a regime where signal amplification is essential. Despite advances in solid-state avalanche gain technologies, the physics of solid-state semiconductors limit the ultimate response time and signal-to-noise ratio (SNR) compared with the fundamental limitations for *in vacuo* electron gain devices, such as the photomultiplier tube (PMT) and microchannel plate (MCP).

PMT and MCP detectors are utilized in many fields of science, from space-based astronomical UV [1] and X-ray observations, to microscopic analysis and diagnosis of *in vivo* biological processes. PMTs are the workhorse detector for photon-counting applications, from medical imaging as PET scanners to detection of exotic particles as neutrino detectors. MCP detectors have the capability to achieve picosecond event timing resolution, and their planar geometry lends itself to high-resolution imaging, with formats exceeding $4000 \times 4000$ pixel$^2$.

The performance of *in vacuo* secondary electron gain devices such as PMTs and MCPs is fundamentally limited by the number of secondary electrons produced by a primary electron impacting the dynode surface. Since the gain progression is geometric, a technology providing improved dynode emission with the stability to use at high signal currents would produce a step advance in the performance. Boron-doped diamond film deposited using chemical vapour deposition (CVD) techniques has been shown to exhibit significantly enhanced secondary electron yield (SEY), especially at higher voltages, compared to traditional dynode materials [2] (see Fig. 1), and its application offers significant advantages:

1. *Enhanced SEY*: Diamond, along with several other high band-gap semiconductors, can exhibit negative electron affinity (NEA) with suitable surface preparation, a major factor enhancing SEY. However, unlike other higher band-gap materials (e.g. AlN, $Ga_{1-y}Al_yN$), synthetic CVD diamond is easy to produce [3].
2. *Simplified design*: Higher SEY results in a lower number of dynodes being required for a given gain, a distinct advantage in terms of device size, cost, and complexity.
3. *Enhanced timing*: Boron-doped (p-type) diamond surfaces produce a narrow energy distribution of low-energy secondary

* Corresponding author. Tel.: +44 116 252 3498; fax: +44 116 252 2464.
*E-mail address:* jsl12@star.le.ac.uk (J.S. Lapington).

0168-9002/$ - see front matter © 2009 Elsevier B.V. All rights reserved.
doi:10.1016/j.nima.2009.05.195

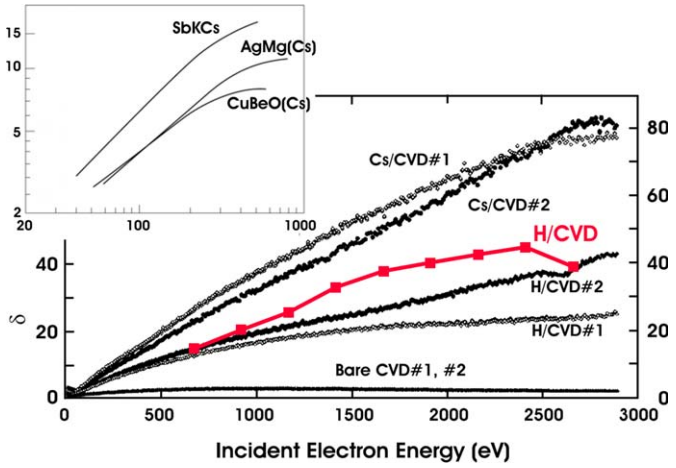


**Fig. 1.** SEY coefficients of three common dynode materials (inset—Photonis PMT Handbook) cf. CVD diamond for different surface terminations [2] and data (grey squares) from our research programme.

electrons [4] allowing improved confinement of trajectories with improved time resolution and reduced background [5].

4. *Narrow pulse height distribution* (*PHD*): The Poisson statistics of high-gain diamond dynodes intrinsically produce a narrower PHD with improved SNR, allowing detector operation at lower gain and better energy resolution for scintillation counters, PET scanners, etc.
5. *Low noise*: Its wide band gap (5.47 eV) precludes the thermal excitation of electrons at typical operating temperatures cf. materials with comparable SEY (e.g. GaP—2.26 eV). Conversely, it has lower thermal noise than traditional dynode materials at high temperatures.
6. *Large-area*: CVD deposition offers a low-cost, large-area coating technique and is applicable to shaped substrates c.f. expensive materials such as GaN and GaP, which can only be grown on lattice matched substrates e.g. sapphire. Inkjet printing of diamond nanoparticles and subsequent growth into patterned films has also been demonstrated.
7. *Stability*: CVD diamond has a stable SEY, little affected by long-term storage. Its SEY remains high after exposure and it can be reactivated [6].

One potential drawback of diamond's higher gain is the increased voltage required per stage. However, diamond's smaller pulse height variance and low noise promote operation at lower gain with a smaller number of stages, thus alleviating the overall voltage requirement.

## 2. Experimental setup

The SEY characterization apparatus is a bakeable stainless-steel vacuum system with a centrally mounted, electrically insulated conductive arm supporting up to four 1 $cm^2$ samples and a small Faraday cup (SFC) for beam current calibration. Fig. 2 shows a schematic diagram of the apparatus and Fig. 3a shows a photograph of the arm with three samples and the SFC aperture.

The sample support arm can be moved laterally by $\pm 25$ mm and rotated 360° around its axis. Lateral motion is used to position one of the samples or the Faraday cup in the path of a beam of electrons generated by an electron gun and rotation allows the beam incidence angle to be varied or the samples placed out of sight of the beam. The ELS5000 electron gun, manufactured by PSP Vacuum Technology [7], produces a focussed electron beam with a spot size of $<50\,\mu$m at 1 μA, working distance of

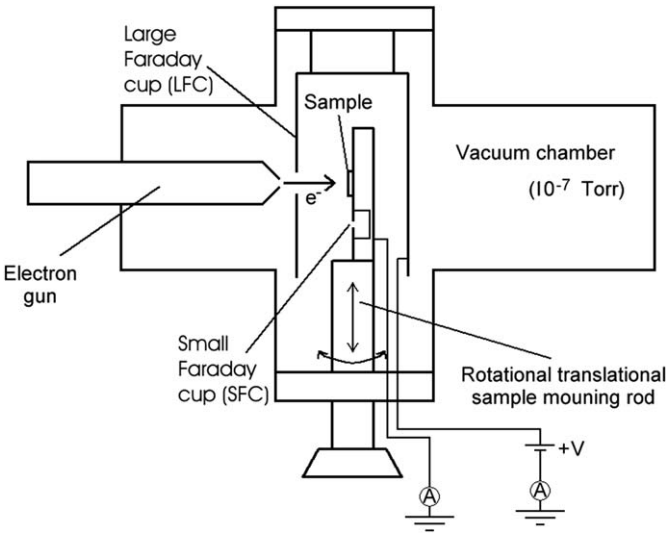


**Fig. 2.** A schematic diagram of the SEY characterization apparatus.

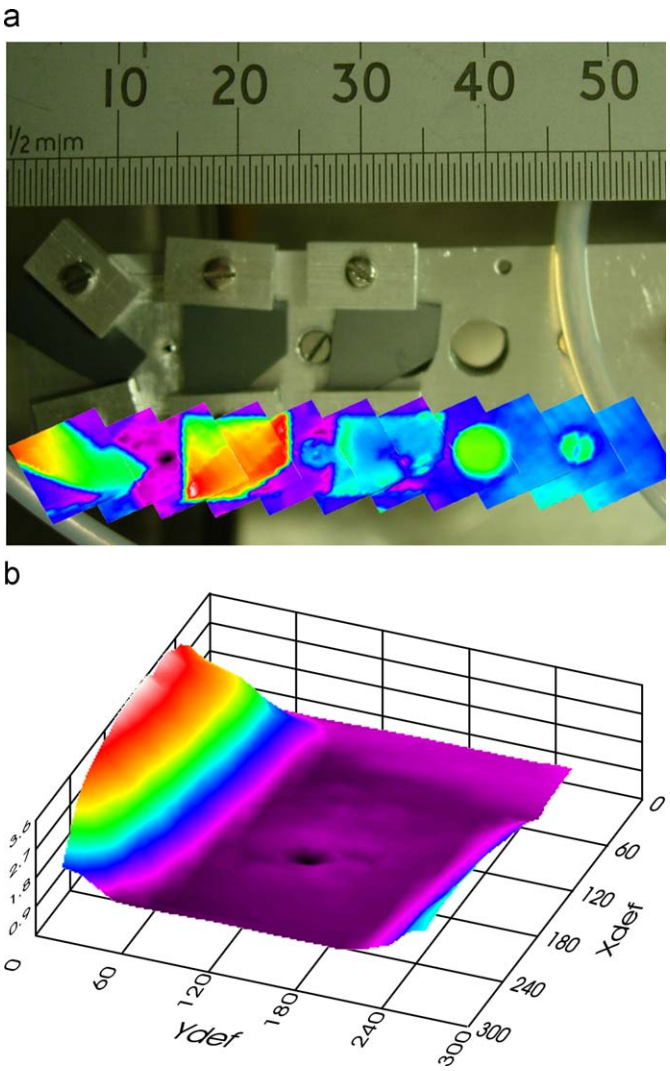


**Fig. 3.** (a). A photograph of the sample arm with three samples. The SFC is the aperture between sample 1 and 2. The montage below is the false colour SEY image produced by scanning the electron beam. Fig. 3b is an SEY image showing the SFC aperture (the black hole in the middle).

15–75 mm, and beam energy of up to 5 keV. The beam can be electrostatically deflected in the *xy* plane by ±5 mm.

Secondary electrons produced by the electron beam impinging the sample are collected by a stainless-steel cylinder, the large Faraday cup (LFC), which surrounds the arm. The LFC is coaxial with the support arm and is mounted on an insulating support at its closed end. The electron beam enters through a small aperture in the side of the LFC. The LFC can (a) be biased and, (b) has extended length to minimize the solid angle of the external chamber seen by emitted secondary electrons from the sample. Both measures serve to ensure secondary electrons from the sample are captured by the LFC. Both the sample support arm and the LFC are electrically insulated allowing them to be biased and their respective collected currents to be measured using a Keithley 6514 Electrometer and 6485 Picoammeter, both operating as precision ammeters. These can be interchanged, however, only the electrometer input can be biased.

Two independent methods can be used to calibrate the electron beam current, (i) the beam can be collected completely in the SFC, the sample current equalling the beam current, confirmed by a zero LFC current, or, (ii) the beam current can be calculated from the sum of sample and LFC currents. The former method requires the electron beam to be sufficiently well focussed to completely pass through the SFC aperture of 0.5 mm. Focussing was carried out by scanning the beam in two dimensions across the SFC aperture using the beam deflection capability, and imaging the aperture by means of the measured SEY, calculated using the sample and LFC currents. The SEY was then given by

$$SEY = \frac{I_{LFC}}{I_{sample} + I_{LFC}} \quad (1)$$

The focus was adjusted to achieve zero SEY over the aperture, the expected result when the beam is fully collected in the SFC. Elsewhere, the phosphor-bronze shim from which the SFC was constructed produced an SEY of ~1.0. This technique also allowed the beam profile to be calculated by deconvolution of the circular SFC pinhole from the imaged SEY (see Fig. 3b).

## 3. Results

Initially the system was pumped with a Leybold turbo pump and rotary backing pump, reaching an ultimate pressure of $\sim 10^{-7}$ mbar. Early on in the experiment it was noted that the measured SEY from any sample material, unless already very low, degraded rapidly over time-scales of minutes as a result of exposure to the electron beam. Evidence in the form of visible contamination, known as electron beam-induced contamination [8], from areas subject to long-term exposure, pointed strongly to the presence of organic contamination. This occurred in two forms, both highly structured, suggesting interaction of the beam with adsorbed contaminants on the sample surface, and as diffuse shadows whose geometry suggested either the presence of a large-angle component in the beam distribution or isotropic evolution of contaminants from a remote source back along the beam line. At this stage the vacuum system was cleaned and the pump set replaced with an oil-free system comprising an Edwards Maglev turbo and scroll pump, though the ultimate vacuum achieved was not appreciably lower.

Another mechanism for SEY degradation is hydrogen desorption from the diamond surface, which causes the disappearance of NEA [9]. Since both electron beam-induced contamination and hydrogen desorption are produced by exposure to the electron beam and are sensitive to total beam flux, they are difficult to distinguish, but their effect can be alleviated if the total flux can be reduced. This approach was used to enable measurement of the nominal SEY of an initially "clean" material. The overall flux was reduced by both pulsing the beam and lowering the beam current. LabView was used for the software platform to automate the measurement procedure, which was used to control the electron gun HV, the *xy* beam deflection, the beam focus, and to initialize and take synchronised measurements from the Keithley ammeters, process the data, and save and display results. Several modes of operation allowed: (1) automated beam focussing, (2) *xy* area beam scan and SEY image capture, (3) energy scan at a single point to produce SEY versus beam energy data, and (4) other calibration procedures. The low-noise Keithley ammeters and good electrical insulation allowed electron beam currents in the 1–10 nA range to be used even when several hundred volt biases were applied to the LFC. The HV was typically pulsed for 0.3 s with the ammeters taking measurements every 10 ms. The time profile of measurements was used to select a window where the currents had reached a stable regime.

These modifications drastically reduced the rate of SEY degradation with total beam charge. Fig. 4 shows a plot of the variation of SEY for a single ~100 μm spot illuminated by the electron beam versus total deposited charge. The contribution of the two SEY degradation mechanisms to this data is uncertain, however, we have qualitative proof that, despite the decontaminated vacuum system and oil-free pump set, electron beam-induced contamination is still present. This is evidenced by

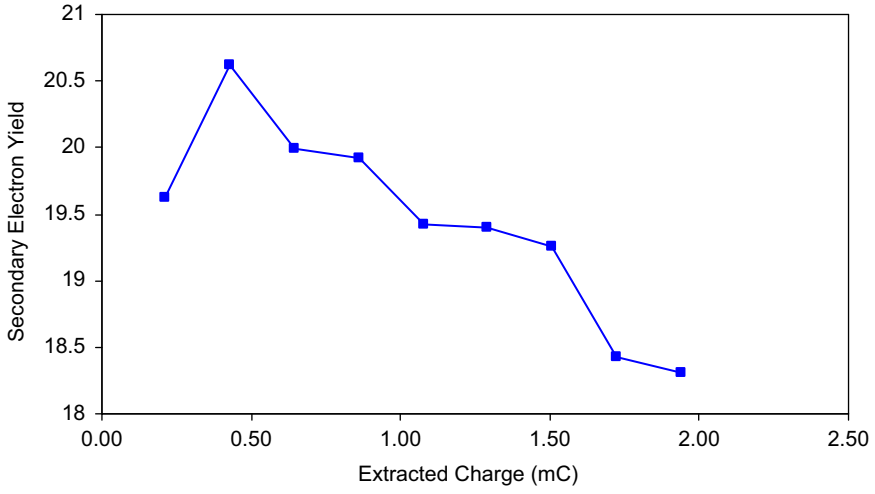


**Fig. 4.** A plot showing the degradation of SEY with increasing electron beam charge.

Fig. 5, which shows a photograph of the SFC after prolonged exposure to the electron beam, producing a diagonal dark stain. However, concurrent SEY imaging of the area around the SFC showed no trace of actual elongation of the beam distribution that this deposit implies. This would be apparent as elongation of the SFC aperture in the SEY image owing to convolution of the beam and aperture distributions.

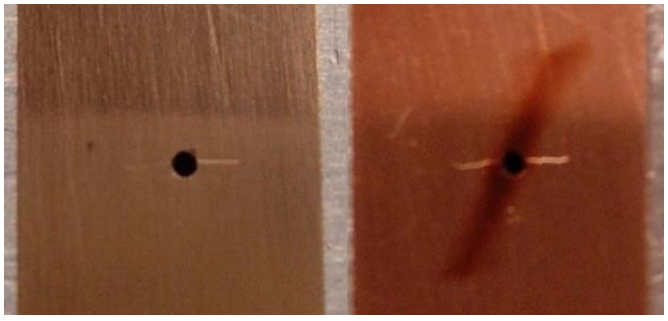

**Fig. 5.** A photograph of the SFC before (left) and after (right) prolonged illumination with the electron beam.

With the apparatus modified to reduce the SEY degradation effects, we measured the SEY of a variety of diamond samples from various sources, manufactured using different methods (CVD, inkjet-printed nanoparticles), dopants and dopant concentrations, and differing crystallinities. Fig. 6 shows a plot of the best results obtained for boron-doped, CVD diamond coated on silicon and molybdenum substrates. The best SEY value so far obtained of 45 for B-doped diamond on silicon at 2.4 keV is the highest reported for hydrogen-terminated material and a strong driver to apply this technology to electron multiplication. However, in the presence of degradation due to electron beam-induced contamination, these must be regarded as preliminary.

However, measurements of variation of SEY with angle of incidence show unexpected behaviour (see Fig. 7). Typically, SEY

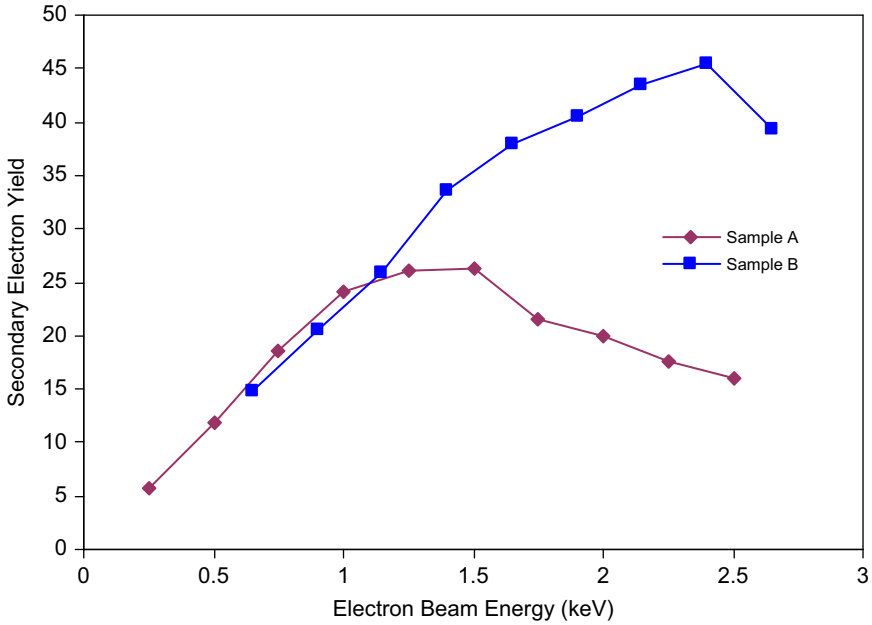


**Fig. 6.** Measured SEY versus beam energy data for hydrogen-terminated B-doped CVD diamond deposited on molybdenum (sample A) and silicon (sample B) substrates.

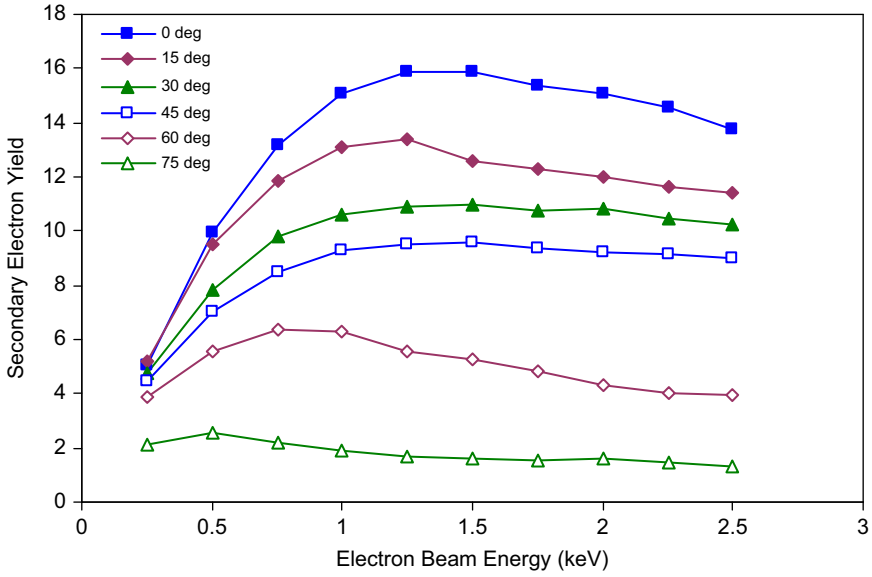


**Fig. 7.** Measured SEY versus energy for hydrogen-terminated B-doped CVD diamond deposited on molybdenum, with the electron beam at various angles of incidence.

is expected to increase with angle of incidence (defined as the angle with respect to the surface normal). This is due to the reduced depth of penetration normal to the surface at higher angles, resulting in an increase in secondary electron escape probability. Either, the high granularity of the surface plays a role in reversing this trend or, as has been suggested by other authors, the secondary electron escape mechanism from polycrystalline diamond is different, utilizing transport along grain boundaries [10].

## 4. Future developments

We have plans to investigate the application of diamond as secondary electron multiplication dynodes in actual detectors operating in two modes:

1. *Transmission*: primary electrons enter through one surface of a thin film of diamond, and secondary electrons exit through the other. Primary track lengths at typical energies coupled with the minority carrier diffusion length requires (a) film thicknesses $<200$ nm, or (b) thicker films with an internal drift field to increase the secondary diffusion length.
2. *Reflection*: diamond is deposited on an open conductive wire mesh or electroformed grid. Primary and secondary electrons enter and exit through the same diamond surface. Coated mesh dynodes (not CVD diamond) are already used in some imaging PMTs.

The transmission technique is conceptually superior, providing a linear detector design with minimum charge spread and guaranteed electron collision at every dynode, ideally suited for imaging applications. It is technologically more demanding; challenges being mechanical support of very thin films or incorporation of internal drift fields.

## 5. Conclusions

We have obtained SEY results from B-doped hydrogen-terminated CVD diamond comparable or better than reported elsewhere. However, we are still encountering electron beam-induced contamination effects within the apparatus and are continuing to develop counter measures to this limitation, while in parallel, attempting to establish the relevance of SEY reduction due to hydrogen desorption. The scale of the latter is the more serious issue, being unavoidable in a detector context in reflection mode. Successful demonstration of high SEY from a transmission dynode will circumvent this problem since hydrogen desorption from the input surface should not affect the NEA of the output surface.

## References

[1] J.S. Lapington, S. Chakrabarti, T. Cook, J.C. Gsell, V.T. Gsell, Nucl. Instr. and Meth. A A513 (2003) 159.
[2] J.E. Yater, A. Shih, R. Abrams, J. Vac. Sci. Technol. A 16 (1998) 913.
[3] P.W. May, Phil. Trans. R. Soc. London A 358 (2000) 473.
[4] J.B. Miller, G.R. Brandes, J. Appl. Phys. 82 (1997) 4538.
[5] Jon Howorth, Photek Ltd., private communication.
[6] G.T. Mearini, I.L. Krainsky, J.A. Dayton Jr., Surf. Interface Anal. 21 (1994) 138.
[7] PSP Vacuum Technology, Macclesfield, UK, 〈www.pspvacuum.com〉.
[8] A.E. Vladar, M.T. Postek, Microsc. Microanal. 11 (Suppl. 2) (2005) 764.
[9] J.B. Cui, J. Ristein, L. Ley, Phys. Rev. B59 (1999) 5847.
[10] J.E. Yater, A. Shih, J.E. Butler, P.E. Pehrsson, J. Appl. Phys. 96 (2004) 446.